Molecular Immunology 65 (2015) 384–390

Contents lists available at ScienceDirect

Molecular Immunology

journal homepage: www.elsevier.com/locate/molimm

Selection and characterization of camelid nanobodies towards urokinase-type plasminogen activator

Jakub Zbigniew Kaczmarek[1], Peter Durand Skottrup*

Department of Drug Design and Pharmacology, Faculty of Health and Medical Sciences, University of Copenhagen, Universitetsparken 2, DK-2100 Copenhagen, Denmark

ARTICLE INFO

Article history:
Received 27 November 2014
Received in revised form 4 February 2015
Accepted 9 February 2015
Available online 6 March 2015

Keywords:
Nanobody
Phage display
Serine protease
Single domain antibody
Antibody technology

ABSTRACT

Urokinase-type plasminogen activator (uPA) is a trypsin-like serine protease that plays a vital role in extracellular conversion of inactive plasminogen into catalytically active plasmin. Activated plasmin facilitates the release of several proteolytic enzymes, which control processes like pericellular proteolysis and remodeling of ECM. uPA and the receptor uPAR, are overexpressed in a number of malignant tumours and uPA/uPAR play major roles in adhesion, migration, invasion and metastasis of cancer cells. Elevated levels of uPA have been reported as a risk biomarker for disease relapse, increased cancer malignancy and poor survival prognosis. For these reasons uPA is considered an important target for anticancer drug therapy.

In this study we isolated two camel single domain antibodies (nanobodies) from a naïve library by phage display. The nanobody sequences were sequence-optimized for *Escherichia coli* expression, cloned into the pET22-B(+) vector system, expressed in BL-21 cells and purified from the periplasmic fraction by IMAC. ELISA tests demonstrated that the purified nanobodies were specific for uPA when tested towards other trypsin-like serine proteases. The apparent affinities of the nanobodies were determined by competitive ELISA to 80 nM and 522 nM, respectively. The best binder did not inhibit uPA (nAb-C3), however the lowest affinity binder (nAb-C8) was able to inhibit the uPA-mediated cleavage of the substrate S-2444.

The results validate the naïve library as a resource for retrieval of relevant lead molecules and the novel uPA-nanobodies can be useful pharmacological tools to study uPA structure–function relationships.

1. Introduction

Containment of cancer cells is one of the biggest problems for efficient treatment. The challenge of limiting cancer spread stems from an inability to efficiently block the production of various growth factors and proteolytic enzymes in the later stages of disease. Proteolytic enzymes lead to neovascularization, tumour growth and promote extracellular matrix (ECM) degradation. These processes combined lead to metastatic spread of primary tumours to distant organs, thus resulting in poor prognosis and high mortality rates (Rabbani and Xing, 1998).

Urokinase-type plasminogen activator (uPA) is a trypsin-like serine protease that plays a crucial role in extracellular conversion of inactive plasminogen into catalytically active plasmin. Together with its cell membrane receptor (uPAR), and two main endogenous inhibitors, the plasminogen activator inhibitor-1 and 2 (PAI-1 and PAI-2), uPA is a part of the urokinase plasminogen activating system. Human uPA has a molecular weight of 54 kDa (411 amino acids) which consists of two α helices and two anti-parallel β strands, and is secreted as a single chain zymogen (pro-urokinase). Upon binding to uPAR, uPA is activated by plasmin through proteolytic cleavage of the Lys_{158}–Ile_{159} peptide bond. The activated two-chain uPA is composed of an A-chain consisting of a kringle-domain and a growth factor domain (GFD) that binds uPAR. The B-chain contains the catalytic domain responsible for enzyme activity and specificity (Spraggon et al., 1995).uPA catalyzes the activation of the zymogen plasminogen into plasmin by proteolytic cleavage. Activated plasmin facilitates the release of several proteolytic enzymes, including gelatinase, fibronectin, fibrin, laminin, collagenases and stromelysins, which control processes like pericellular proteolysis and remodelling of ECM (Vincenza Carriero

* Corresponding author. Present address: Department of Clinical Biochemistry, Copenhagen University Hospital, Kettegård Allé 30, DK-2650 Hvidovre, Denmark. Tel.: +45 38620117.
E-mail address: peter.durand.skottrup@regionh.dk (P.D. Skottrup).
[1] Current address: Research and Development Department, Sanovo Biotech A/S, DK-5000 Odense, Denmark.

http://dx.doi.org/10.1016/j.molimm.2015.02.011
0161-5890/

et al., 2009). uPA and uPAR, are overexpressed in several types of malignant tumours, such as breast, prostate and glioblastoma, colon, renal cell, hepatocellular and pancreatic (de Witte et al., 1999; Hsu et al., 1995; Mizukami et al., 1994; Paciucci et al., 1998). uPA/uPAR play major roles in adhesion, migration, invasion and metastasis of cancer cells. Elevated levels of uPA, and the inhibitor PAI-1, have been reported as risk biomarker for disease relapse, increased cancer malignancy and poor survival prognosis (Duffy, 2002; Duffy and Duggan, 2004). For the reasons above uPA is considered an important target for anticancer drug therapy (Dass et al., 2008).

Members of the camelid family (camel—*Camelus bactrianus*, dromedary—*Camelus dromedarius*, llama—*Lama glama* and alpaca—*Vicugna pacos*) produce antibodies (Abs) with no associated light chains named heavy chain antibodies (Harmsen and De Haard, 2007). Libraries of single domain antibodies derived from these heavy chains (VHH's, also termed nanobodies) can be constructed by the use of molecular biology methods and by display techniques it has been possible to develop nanobodies (nAbs) for diagnostic and therapeutic applications (De Meyer et al., 2014). nAbs are small (~15 kDa) and stable molecules, which can be recombinantly produced in several host cells (Muyldermans et al., 2009). Traditional heavy-light chain antibodies have a concave paratope formed by the six CDR's found on the heavy chain and light chain. However, nAbs only have three CDR's resulting in a paratope with a convex structure, which have a preference for binding epitopes located in surface crevices (De Genst et al., 2006). Furthermore, the relative small size of nAbs makes them efficient in penetration of dense tumour tissue (Revets et al., 2005). Indeed, a nanobody targeting the epidermal growth factor receptor has been found to efficiently inhibit tumour growth *in vivo* (Roovers et al., 2007). For these reasons nAbs can be interesting molecules for uPA inhibition by targeting the uPA active site or other crevices on the molecule leading to enzyme inhibition. In this study were have therefore isolated uPA-binding nanobodies and further characterized their properties.

2. Materials and methods

2.1. Panning

Purified human uPA (US Biological) was immobilized on maxisorp wells (Nunc) overnight in PBS (20 mM sodium phosphate, 150 mM NaCl, pH 7.4) at 4 °C for panning experiments (50 μg/ml). Wells were washed 3 times in PBS and blocked in 4% (w/v) skimmed milk powder/PBS for 1 h. Wells were washed three times with PBS-T (PBS with 0.05% Tween20). The production of the naïve camel nanobody library used in the study is described elsewhere (Skottrup et al., 2011). Coated and blocked wells were incubated for 2 h with approximately 10^{11} nanobody-phage in 2% (w/v) skimmed milk powder/PBS. Wells were washed 15 times in PBS-T and phages were eluted with 100 μl 10 mM glycine–HCl pH 2.0 for 10 min followed by addition of 1 μl 2 M TRIS-base for neutralization. The eluate was used to infect exponentially growing TG1 cells for 20 min. Next 100 μg/ml ampicillin (Calbiochem) was added to the LB-media (Sigma-Aldrich) and the culture was incubated overnight at 37 °C. From the overnight culture nanobody-phage were produced by adding a 100-fold excess of the R408 helper phages (Promega), followed by culture incubation for 20 min at 37 °C and induction with 1 mM isopropyl β-D-thiogalactoside (IPTG, VWR) overnight at 22 °C. The following day nanobody-phage were precipitated from the cell supernatant with phage precipitation buffer (20% (w/v) PEG6000), 2.5 M NaCl) and redissolved in PBS. The nanobody-phage fraction was used for the next panning round and stored at −20 °C.

2.2. Clone screening by phage ELISA

Single clones were isolated and superinfected for nanobody-phage production overnight as described above. Overnight cultures were centrifuged at 10,000 × *g* to remove cells and the supernatants were diluted 1:1 in 4% (w/v) skimmed milk powder/PBS and applied directly to uPA-coated and blocked maxisorp wells (coating concentration was 50 μg/ml). The nanobody-phage were incubated for 2 h at room temperature followed by washing 5 times with PBS-T. Nanobody-phage binding was detected by a monoclonal anti-M13 antibody-HRP conjugate (diluted 1/1000, GE-healthcare) and OPD as the substrate (Dako).

2.3. Nanobody expression and purification

Expression of nAb-C3 and nAb-C8 were attempted in three ways. First, pFab74 phagemid harboring the nAb-C3 and nAb-C8 sequences fused to protein III was isolated by miniprep (QIAgen). The phagemids were digested with the restriction enzyme *Eag*I (New England Biolabs) to remove the protein III sequence (Engberg et al., 2003) and expressed in TG1 cells as described (Skottrup et al., 2011). In the second alternative, sequences were PCR amplified from the pFab74 phagemid (for both C3 and C8) and cloned into the pET22B(+) vector followed by transformation into BL21 (DE3) *Escherichia coli* cells (Life Technologies). Cells were expanded in LB-media (supplemented with 100 μg/ml ampicillin) to OD_{600} = 0.8, and induction was started with 1 mM IPTG for 16 h at 30 °C. The periplasmic fraction was isolated according to (Skottrup et al., 2011) and extensively dialysed into 20 mM sodium phosphate, 500 mM NaCl, pH 7.4 (buffer A). In the third method synthetic genes (codon optimized for *E. coli*) were used. These were cloned into pET22-B(+) and transformed into BL21 (DE3). Expression, periplasmic fraction extraction and dialysis were performed as described above. The dialysed C3-nAb and C8-nAb fractions were applied to 1 ml HiTrap chelating HP columns charged with $NiSO_4$ (GE Healthcare). The hexa-His tagged nAbs were eluted from columns using a linear gradient of buffer B (20 mM sodium phosphate, 500 mM NaCl, 500 mM imidazole, pH 7.4). Purity of C3-nAb and C8-nAb were confirmed by SDS–PAGE. Samples were concentrated using 15 ml 10 kDa cut-off spin columns (Millipore) and buffer exchanged into PBS-buffer using PD-10 columns (GE Healthcare).

2.4. Estimated binding affinity by inhibition ELISA

Nunc maxisorp plates were coated with 10 μg/ml uPA and blocked with 4% (w/v) skimmed milk powder/PBS as described in Section 2.2. A titration curve revealed the nAb-C3 and nAb-C8 concentrations that gave half maximum response and these concentrations were used for the inhibition assay. The inhibition assay was performed essentially as previously described (Rath et al., 1988). Briefly, the nAb was incubated with decreasing concentrations of uPA for 1 h with extensive mixing. The mix was added to coated/blocked wells (10 μg/ml uPA) and the unbound nAb was allowed to bind for 1 h. Wells were washed with PBS-T five times and incubated with rabbit anti-camel whole serum pAb (Bethyl laboratories, diluted 1/1000) for 1 h, followed by PBS-T washing five times. The final step was incubation with a goat anti-rabbit IgG-HRP conjugate (diluted 1/1000, Sigma-Aldrich) for 1 h and development with TMB substrate (Dako). The absorbance values were measured at 450 nm after 30-min incubation at 22 °C. Absorbance values at each uPA concentration (A) were divided by the absorbance measured in the presence of zero uPA (A_0), which yielded normalized values (A/A_0). The normalized values were plotted against the uPA concentration to construct the inhibition curve. The assay was performed in triplicate measurements to generate standard deviations. The uPA concentration required for 50% inhibition was identified

and used as an estimated antibody affinity as described previously (Rath et al., 1988). Data analysis was performed with GraphPad prism.

2.5. ELISA for determination of cross reactivity with other serine proteinases

To determine cross-reactivity of the uPA-nanobodies towards other trypsin-like serine proteases an ELISA test was performed using thrombin (Sigma-Aldrich), chymotrypsin B (Sigma-Aldrich), trypsin (Sigma-Aldrich), tPA (Aniara) and plasmin (Sigma-Aldrich) as the antigen. The proteases were coated in maxisorp plates at concentrations corresponding to the 10 μg/ml uPA (185 nM). Wells with 10 μg/ml uPA pre-incubated with 1 mM Benzamidine (Sigma-Aldrich) for 30 min prior to coating were also included. The binding of benzamidine to uPA was verified in functional assays, where the uPA–benzamidine complex was inactive towards S2444. The Plate was blocked as described in Section 2.5 and nAb-C3 and nAb-C8 were diluted in PBS-T to C3; 200 ng/ml and C8; 600 ng/ml and applied to all wells. Incubation was performed for 1 h. Wells were washed with PBS-T five times and incubated with rabbit anti-camel whole serum pAb (Bethyl laboratories, diluted 1/1000) for 1 h, followed by PBS-T washing five times. The final step was incubation with a goat anti-rabbit IgG-HRP conjugate (diluted 1/1000, Sigma-Aldrich) for 1 h and development with TMB substrate (Dako). The absorbance values were measured at 450 nm after 30-min incubation at 22 °C.

2.6. uPA activity assay

The uPA activity assay using S-2444 L-pyroglutaminyl-glycyl-L-arginine-*p*-nitroalinine hydrochloride (chromogenix) was performed essentially as described (Petersen et al., 2001). Briefly, 100 nM uPA was incubated with various concentrations of purified nAb-C3 and nAb-C8 (31–4000 nM) in 2.5 mM NaH_2PO_4, 35 mM NaCl, 75 mM Tris/HCl, 0.2% Triton X-100, pH 8.1. After a 30 min pre-incubation of uPA and nanobody, the substrate S-2444 was added in a final concentration of 0.4 mM and colour formation was allowed to develop for 60 min, followed by plate reading at 405 nm. Data was plotted and analysed using GraphPad prism.

2.7. Test for overlapping epitopes

The nanobodies were biotinylated individually using Biotinamidohexanoic acid *N*-hydroxysuccinimide ester (Sigma-Aldrich). A microtiter plate was coated with uPA and blocked as described in Section 2.5. The biotinylated nAbs were titrated over immobilized uPA to find the half maximal OD-value suitable for competitive assays. For the competitive assay biotinylated nAb-C3 and biotinylated nAb-C8 were individually incubated with uPA-coated microtiter wells in the presence of varying concentrations of unlabeled nAb-C3 and nAb-C8, respectively (0.06–1 μM). The plate was incubated for 1 h on a vertical shaker. Wells were washed with PBS-T five times and incubated with streptavidin-HRP (Sigma-Aldrich, diluted 1/1000) for 1 h, followed by PBS-T washing five times. Assay development was with TMB substrate for 30 min (Dako).

3. Results and discussion

3.1. Panning with nanobody library on immobilised uPA

This study explored our in-house naïve camel nanobody library for binders towards purified human uPA. Following 5 panning rounds we screened 48 clones and were able to isolate two phage positive for uPA-binding in phage-ELISA (data not shown). The selected phage were named nAb-C3 and nAb-C8. Phage-DNA was extracted and sequencing revealed that the two nAb's had unique sequences (Fig. 1A). The nAb-C3 had an uncharacteristic short CDR3 and no cysteine residues in CDR1 and CDR3. The nAb-C8 binder had a relatively long CDR3 loop of 19 amino acids. Furthermore, cysteine residues were found in both CDR1 and CDR3, suggesting that a disulfide bridge could stabilize the long CDR3 loop, which is a general trend seen in camelid nanobodies (Muyldermans, 2013).

3.2. Nanobody expression and purification

Initially, expression was attempted directly from the pFab74 phagemid vector as described (Skottrup et al., 2011) and using this method approximately 0.25 mg/L IMAC-pure RgpB-nanobody was obtained. In the case of nAb-C3 and nAb-C8, only minute amounts of nanobody were found in the periplasmic fraction and we were not able to achieve expression levels suitable for IMAC purification. Instead, we PCR cloned the sequences into the pET22-B(+) vector and transformed BL21 (DE3) cells. After validation of the correct inserts by sequencing, we induced expression and 3 h later the periplasmic fraction was isolated. However, again, the obtained expression levels were too low for large scale IMAC purification as only a faint protein band was seen on SDS–PAGE. When combining the two expression procedures above with having attempted two very different expression systems, it was speculated that that the low yields were sequence-induced. Therefore, the sequences were optimized for *E. coli* expression, cloned into pET22-B(+) and expressed in BL21 (DE3). Using this system it was possible to achieve satisfactory expression levels and following a one-step IMAC purification yields of 3.5 mg nAb-C3 and 2.1 mg nAb-C8 (both from 5 l *E. coli* culture were obtained (Fig. 1B). Two smaller bands were found in the nAb-C8 preparation, which were likely nanobody degradation products.

Higher nAb-yields have been reported in the literature. Habib et al. (2013) were able to achieve expression levels of 100 mg/ml using *E. coli* shuffle cells. In addition, nAbs have been successfully produced in large scale by the use of *Pichia pastoris*, *Saccharomyces cerevisiae* and *Aspergillus awamori* (Frenken et al., 2000; Joosten et al., 2005; Rahbarizadeh et al., 2006; Thomassen et al., 2005; van der Vaart, 2002). The yields of nAb-C3 and nAb-C8 obtained were acceptable for further nanobody characterization, but it is likely that the alternative expression systems described above can be pursued for higher yields.

3.3. Estimated nanobody affinity by inhibition ELISA

The apparent binding affinity was identified for both nAb-C3 and nAb-C8 using an inhibition ELISA method described previously (Rath et al., 1988). Inhibition curves can be seen in Fig. 2 and from these data apparent affinities were calculated. The nAb-C3 was found to have a good binding affinity of approximately 80 nM, whereas nAb-C8 had a low affinity of approximately 522 nM. The nAb-C3 had an acceptable affinity similar to what has been seen earlier. However, the nAb-C8 could likely be improved by affinity maturation. Indeed, due the simpler single chain (only three CDR's) of nanobodies, affinity maturation is less complicated than affinity maturation of scFv's. Shahi et al. (2014) have recently, improved nanobody affinity by error prone PCR. These authors were able to create a secondary library and achieved a 10% affinity improvement over the parental nanobody. Similarly by error-prone PCR Hoseinpoor et al. (2014) were able to improve the binding affinity of a nanobody towards *Helicobacter pylori* urease by 1.5-fold compared to the original VHH ().

Using our in-house naïve camel nanobody library we have earlier identified a binder with picomolar affinity (Skottrup et al., 2011) and several micromolar affinity binders towards various targets

A

Clone name	CDR1	CDR2	CDR3
nAb-C3	GITGTTTIPGWMY	INTHTGIPYWPDSSMAD	DKDGKG
nAb-C8	QASGYMY**C**TYAVT	AIDSGDNRTYYADSVNG	DPTWDDGY**C**YELNEESFGS

B

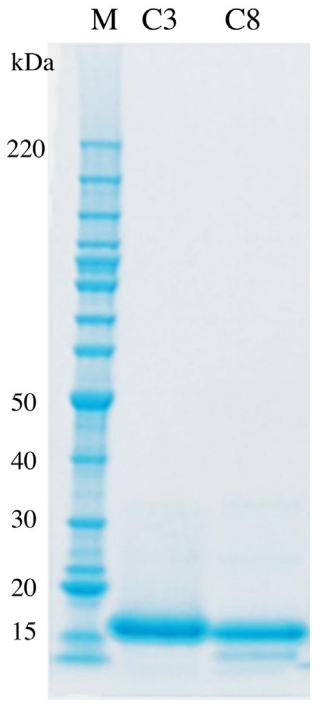

Fig. 1. *Purity of nAb-C3 and nAb-C8 following IMAC purification and CDR sequences*. (A) Shown are CDR1-3 for each identified nAb. CDR's were identified using the recently published guidelines (Sircar et al., 2011). In nAb-C8 cysteine residues are underlined, which likely represent a disulfide bridge for CDR3 stabilization. (B) SDS–PAGE analyses using ten micrograms of protein was used to confirm nanobody purity. The nanobodies were found to be more than 90% pure. The molecular weight marker (M) is Benchmark™ Pre-stained protein ladder.

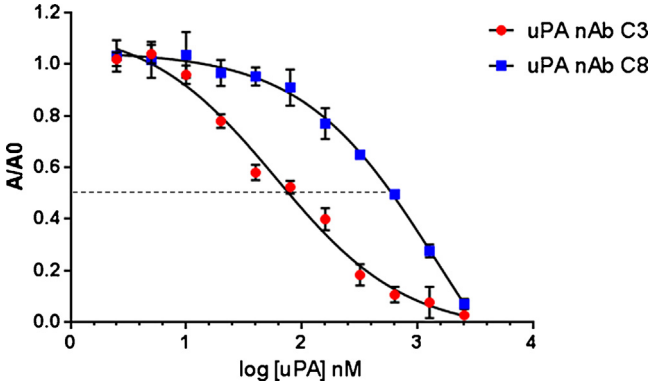

Fig. 2. *Competitive ELISA for estimation of nanobody apparent affinity*. nAb-C3 and nAb-C8 were pre-incubated with increasing concentration of uPA and the remaining unbound nanobodies were analysed as described in materials and methods. Normalised responses (A/A_0) for increasing concentrations of uPA are shown. Data represents three assays performed on the same day with error bars to depict standard deviations. Each data set is fitted to a logistic 4-parameter equation and the apparent binding affinites were estimated to 80 nM (nAb-C3) and 522 nM (nAb-C8). A dotted line indicating the IC50 value is seen in the graph. GraphPad prism was used for data analyses.

(unpublished data). Recently, a naïve llama library was panned on six different protein targets thereby demonstrating high throughput screening for binders (Monegal et al., 2009). The resulting nanobodies had binding affinities ranging from 0.15 to 1970 nM, which is comparable to what we observed when extracting binders from our library. Not surprisingly, we conclude that binder affinity is protein dependent, which is similar to the conclusion of Monegal et al. (2009).

3.4. Nanobody specificity

Direct ELISA was used to determine the degree of cross-reactivity of nAb-C3 and nAb-C8 towards other trypsin-like serine proteases (Fig. 3). When tested towards thrombin, chymotrypsin, trypsin, tPA and plasmin both nanobodies were specific for uPA-binding, thereby demonstrating that they bind epitopes unique to uPA. Wells with benzamidine-inhibited uPA were also included in the ELISA study. Benzamidine is a broad specificity arginine mimetic that interacts with the negatively charged aspartate at the bottom of the S1 pocket of trypsin and trypsin-like serine proteases such as thrombin, plasmin and uPA. Benzamidine therefore acts

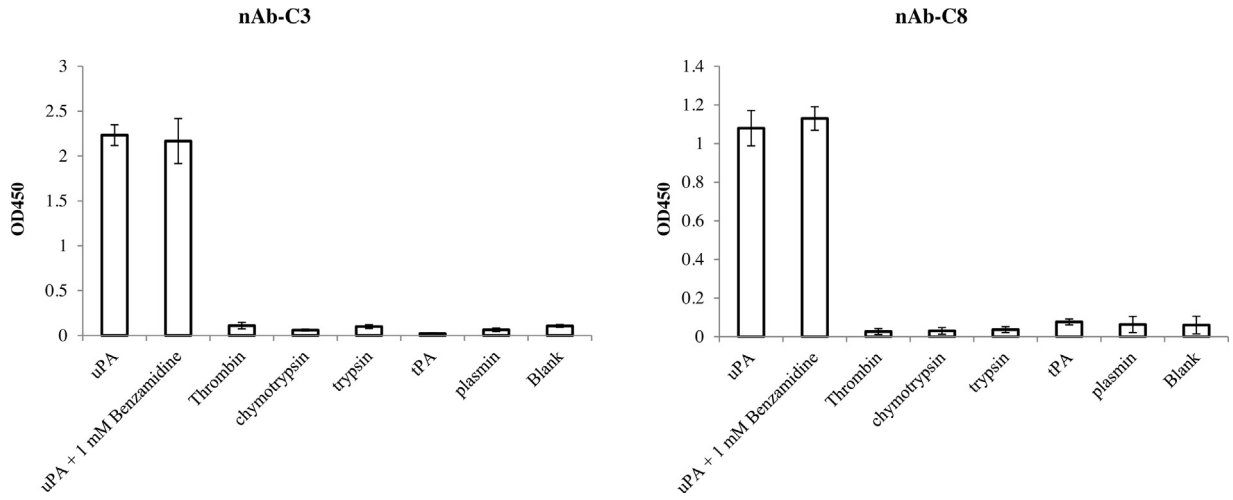

Fig. 3. *Cross reactivity profiles of uPA nAbs.* The nAb-C3 and nAb-C8 were tested in direct ELISA for binding towards other serine proteases. The nAbs bound exclusively to uPA. Interestingly, when tested for binding towards Benzamidine-inhibited uPA good binding was observed, thereby suggesting that the nAbs do not bind the uPA active site. Data represents triplicate analysis with error bars to depict standard deviations.

the role of a reversible competitive inhibitor by interfering with the protease catalytic mechanism (Renatus et al., 1998; Zeslawska et al., 2000). Interestingly, when the nanobodies were tested towards benzamidine-inhibited uPA, full binding was observed (Fig. 3). The binding of benzamidine to uPA was verified in functional assays, where the uPA-benzamidine complex was inactive towards S2444, thereby confirming that the nAbs did indeed bind an uPA–benzamidine complex. Therefore, the fact that both nAb binds the uPA–benzamidine complex excludes the possibility that nAbs bind uPA by active site targeting.

3.5. Performance of the nanobodies in uPA-functional assays

The uPA activity was monitored using the chromogenic substrate S-2444. The commercial preparation of uPA reacted relatively slow on the S-2444 substrate so a concentration of 100 nM uPA was used in the assay to obtain sufficient OD-values. Both nAb-C3 and nAb-C8 were tested for inhibition towards uPA in this functional assay. As seen in Fig. 4 the high affinity antibody C3 was not able to inhibit the uPA activity and displayed a profile similar to the control nanobody towards RgPB (VHH7). However, the nAb-C8 did display a clear dose-response inhibition profile towards uPA and the IC50 was found to be approximately 788 nM. This result taken together with the finding that nAb-C8 does not bind the uPA active site suggest that the inhibition mechanism is allosteric.

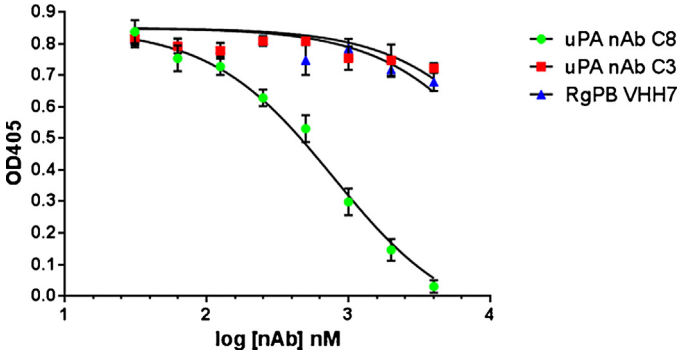

Fig. 4. *nAb-C8 inhibits the proteolytic activity of uPA but nAb-C3 does not.* As can be seen in the figure nAb-C8 inhibits the activity of uPA in a dose-response manner within the concentration range tested (31–4000 nM). A log [nAb] *x*-axis is used. nAb-C3 is unable to inhibit uPA and behaves similarly as the RgPB nanobody VHH7 negative control. Data represents three assays performed on the same day with error bars to depict standard deviations. The uPA activity in the presence of no nAb was found to be OD450 = 0.82 ± 0.03 (n = 6). Each data set was fitted to a logistic 4-parameter equation and the nAb-C8 IC50 was found to be approximately 788 nM. GraphPad prism was used for data analyses.

To investigate whether the two nAbs had overlapping binding epitopes on uPA, we performed competitive ELISA assays using biotin-labelled nAb-C3 and nAb-C8, respectively. We found that only nAb-C3 was able to outcompete the binding of biotinylated nAb-C3 (Fig. 5A). The same trend was observed in Fig. 5B, where only nAb-C8 was able to outcompete the binding of biotinylated nAb-C8. Therefore it was concluded that the binding epitopes are not completely or partially overlapping.

Several different molecules have been developed for the purpose of uPA inhibition, including peptides isolated from phage display libraries (Andersen et al., 2008; Hansen et al., 2005), a polyclonal antibody (pAb) (Dano et al., 1980), monoclonal antibodies (mAb) (Kaltoft et al., 1982; Petersen et al., 2001) and low molecular weight organochemical inhibitors (Mackman et al., 2001; Magdolen et al., 2000; Sperl et al., 2000; Zeslawska et al., 2000). The peptides identified are very specific for uPA and have K_D's in the high nanomolar range. The pAb and mAbs isolated so far are specific but do not completely inhibit uPA activity towards low molecular weight substrates. A recent study also showed that a human recombinant antibody selected from a commercial library could inhibit the enzymatic activity of uPA with dissociation constant and IC_{50} values in the low nanomolar range (Sgier et al., 2010). Organochemical inhibitors are highly effective for uPA inhibition, but they lack specificity as they often inhibit other serine proteases as well (Mackman et al., 2001; Magdolen et al., 2000; Sperl et al., 2000; Zeslawska et al., 2000).

Compared to conventional antibodies, nAbs are capable of targeting epitopes deeper in protein structures as nAbs are less sterically hindered in the interaction with ligands. Consequently, nAbs are a completely new class of biomolecules that are antibody-derived, but bind target proteins in a novel way. nAbs have proved to be very efficient as protease inhibitors and several nAbs that act by enzyme active site targeting have been isolated (Chan et al., 2008; Conrath et al., 2009; Dong et al., 2010; Thanongsaksrikul et al., 2010). Similarly, nAbs have been selected for cell surface receptor antagonism and as inhibitors of receptor function (Ahmadvand et al., 2009; Roovers et al., 2007). The binding epitope of the inhibitory nAb-C8 is distant from the uPA active site and therefore acts as an allosteric inhibitor. Future, epitope

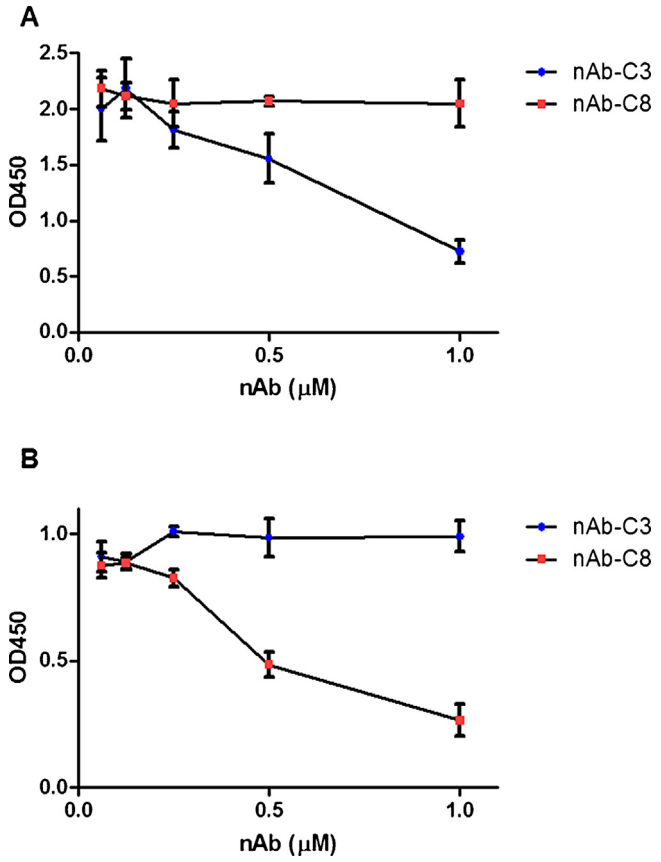

Fig. 5. *The uPA nAbs do not bind overlapping epitopes on uPA.* (A) nAb-C3 was biotinylated and binding to immobilized uPA was monitored by streptavidin-HRP in the presence of increasing concentrations of unlabelled nAb-C3 or nAb-C8. Only unlabelled nAb-C3 was able to outcompete biotin-nAb-C3. (B) nAb-C8 was biotinylated and binding to immobilized uPA was monitored by streptavidin-HRP in the presence of increasing concentrations of unlabelled nAb-C3 or nAb-C8. Only unlabelled nAb-C8 was able to outcompete biotin-nAb-C8. Taken together these results demonstrate that nAb-C3 and nAb-C8 do not have overlapping epitopes. Data represents duplicate analysis with error bars to depict standard deviations.

mappings of this novel nanobody can elucidate the binding mechanism and the nanobody could be used as valuable biochemical tool in structure–function studies of uPA.

4. Conclusion

In this paper we successfully selected two nanobodies towards uPA from a naïve camel library. We were able to express the nanobodies in *E. coli*. The purified nAbs were characterized in terms of their affinity towards uPA and did not share a common binding epitope on uPA. The nAb-C8 was found to inhibit the uPA activity towards a small molecule substrate and this nanobody was furthermore specific for uPA, when tested towards other trypsin-like proteases. Finally we were able to demonstrate that nAb-C8 does not inhibit uPA by active site binding, thereby suggesting that nAb-C8 targets an epitope that induces allosteric inhibition. In conclusion, the uPA-nanobodies can be useful pharmacological tools to study uPA structure–function relationships.

Acknowledgements

PDS wishes to thank the Lundbeck Foundation for financial support. We wish to thank Grete Sørensen for excellent technical assistance.

References

Ahmadvand, D., Rasaee, M.J., Rahbarizadeh, F., Kontermann, R.E., Sheikholislami, F., 2009. Cell selection and characterization of a novel human endothelial cell specific nanobody. Mol. Immunol. 46, 1814–1823.
Andersen, L.M., Wind, T., Hansen, H.D., Andreasen, P.A., 2008. A cyclic peptidylic inhibitor of murine urokinase-type plasminogen activator: changing species specificity by substitution of a single residue. Biochem. J. 412, 447–457.
Chan, P.H., Pardon, E., Menzer, L., De Genst, E., Kumita, J.R., Christodoulou, J., Saerens, D., Brans, A., Bouillenne, F., Archer, D.B., Robinson, C.V., Muyldermans, S., Matagne, A., Redfield, C., Wyns, L., Dobson, C.M., Dumoulin, M., 2008. Engineering a camelid antibody fragment that binds to the active site of human lysozyme and inhibits its conversion into amyloid fibrils. Biochemistry 47, 11041–11054.
Conrath, K., Pereira, A.S., Martins, C.E., Timoteo, C.G., Tavares, P., Spinelli, S., Kinne, J., Flaudrops, C., Cambillau, C., Muyldermans, S., Moura, I., Moura, J.J.G., Tegoni, M., Desmyter, A., 2009. Camelid nanobodies raised against an integral membrane enzyme, nitric oxide reductase. Protein Sci. 18, 619–628.
Dano, K., Nielsen, L.S., Moller, V., Engelhart, M., 1980. Inhibition of plasminogen-activator from oncogenic virus-transformed mouse cells by rabbit antibodies against the enzyme. Biochim. Biophys. Acta 630, 146–151.
Dass, K., Ahmad, A., Azmi, A.S., Sarkar, S.H., Sarkar, F.H., 2008. Evolving role of uPA/uPAR system in human cancers. Cancer Treat. Rev. 34, 122–136.
De Genst, E., Silence, K., Decanniere, K., Conrath, K., Loris, R., Kinne, J., Muyldermans, S., Wyns, L., 2006. Molecular basis for the preferential cleft recognition by dromedary heavy-chain antibodies. Proc. Natl. Acad. Sci. U.S.A. 103, 4586–4591.
De Meyer, T., Muyldermans, S., Depicker, A., 2014. Nanobody-based products as research and diagnostic tools. Trends Biotechnol. 32, 263–270.
de Witte, J.H., Sweep, C.G., Klijn, J.G., Grebenschikov, N., Peters, H.A., Look, M.P., van Tienoven, T.H., Heuvel, J.J., van Putten, W.L., Benraad, T.J., Foekens, J.A., 1999. Prognostic impact of urokinasetype plasminogen activator (uPA) and its inhibitor (PAI-1) in cytosols and pellet extracts derived from 892 breast cancer patients. Br. J. Cancer 79, 1190–1198.
Dong, J., Thompson, A.A., Fan, Y., Lou, J., Conrad, F., Ho, M., Pires-Alves, M., Wilson, B.A., Stevens, R.C., Marks, J.D., 2010. A single-domain llama antibody potently inhibits the enzymatic activity of botulinum neurotoxin by binding to the non-catalytic alpha-exosite binding region. J. Mol. Biol. 397, 1106–1118.
Duffy, M.J., 2002. Urokinase plasminogen activator and its inhibitor, PAI-1, as prognostic markers in breast cancer: from pilot to level 1 evidence studies. Clin. Chem. 48, 1194–1197.
Duffy, M.J., Duggan, C., 2004. The urokinase plasminogen activator system: a rich source of tumour markers for the individualised management of patients with cancer. Clin. Biochem. 37, 541–548.
Engberg, J., Yenidunya, A.F., Clausen, R., Jensen, L.B., Sørensen, P., Kops, P., Riise, E., 2003. Human recombinant Fab antibodies with T-cell receptor-like specificities generated from phage display libraries. Methods Mol. Biol. 207, 161–177.
Frenken, L.G., van der Linden, R.H., Hermans, P.W., Bos, J.W., Ruuls, R.C., de Geus, B., Verrips, C.T., 2000. Isolation of antigen specific llama VHH antibody fragments and their high level secretion by *Saccharomyces cerevisiae*. J. Biotechnol. 78, 11–21.
Habib, I., Smolarek, D., Hattab, C., Grodecka, M., Hassanzadeh-Ghassabeh, G., Muyldermans, S., Sagan, S., Gutierrez, C., Laperche, S., Le-Van-Kim, C., Aronovicz, Y.C., Wasniowska, K., Gangnard, S., Bertrand, O., 2013. V(H)H (nanobody) directed against human glycophorin A: a tool for autologous red cell agglutination assays. Anal. Biochem. 438, 82–89.
Hansen, M., Wind, T., Blouse, G.E., Christensen, A., Petersen, H.H., Kjelgaard, S., Mathiasen, L., Holtet, T.L., Andreasen, P.A., 2005. A urokinase-type plasminogen activator-inhibiting cyclic peptide with an unusual P-2 residue and an extended protease binding surface demonstrates new modalities for enzyme inhibition. J. Biol. Chem. 280, 38424–38437.
Harmsen, M.M., De Haard, H.J., 2007. Properties, production, and applications of camelid single-domain antibody fragments. Appl. Microbiol. Biotechnol. 77, 13–22.
Hoseinpoor, R., Mousavi Gargari, S.L., Rasooli, I., Rajabibazl, M., Shahi, B., 2014. Functional mutations in and characterization of VHH against *Helicobacter pylori* urease. Appl. Biochem. Biotechnol. 172, 3079–3091.
Hsu, D.W., Efird, J.T., Hedley-Whyte, E.T., 1995. Prognostic role of urokinase-type plasminogen activator in human gliomas. Am. J. Pathol., 147.
Joosten, V., Gouka, R.J., van den Hondel, C.A., Verrips, C.T., Lokman, B.C., 2005. Expression and production of llama variable heavy-chain antibody fragments (V(HH)s) by *Aspergillus awamori*. Appl. Microbiol. Biotechnol. 66, 384–392.
Kaltoft, K., Nielsen, L.S., Zeuthen, J., Dano, K., 1982. Monoclonal antibody that specifically inhibits a human MR 52,000 plasminogen-activating enzyme. Proc. Natl. Acad. Sci. U.S.A.—Biol. Sci. 79, 3720–3723.
Mackman, R.L., Katz, B.A., Breitenbucher, J.G., Hui, H.C., Verner, E., Luong, C., Liu, L., Sprengeler, P.A., 2001. Exploiting subsite S1 of trypsin-like serine proteases for selectivity: potent and selective inhibitors of urokinase-type plasminogen activator. J. Med. Chem. 44, 3856–3871.
Magdolen, V., de Prada, N.A., Sperl, S., Muehlenweg, B., Luther, T., Wilhelm, O.G., Magdolen, U., Graeff, H., Reuning, U., Schmitt, M., 2000. Natural and synthetic inhibitors of the tumor-associated serine protease urokinase-type plasminogen activator. Adv. Exp. Med. Biol. 477, 331–341.
Mizukami, I.F., Garni-Wagner, B.A., DeAngelo, L.M., Liebert, M., Flint, A., Lawrence, D.A., Cohen, R.L., Todd 3rd., R.F., 1994. Immunologic detection of the cellular receptor for urokinase plasminogen activator. Clin. Immunol. Immunopathol. 71, 96–104.

Monegal, A., Ami, D., Martinelli, C., Huang, H., Aliprandi, M., Capasso, P., Francavilla, C., Ossolengo, G., de Marco, A., 2009. Immunological applications of single-domain llama recombinant antibodies isolated from a naïve library. Protein Eng., Des. Sel. 22, 273–280.

Muyldermans, S., 2013. Nanobodies: natural single-domain antibodies. Annu. Rev. Biochem. 82, 775–797.

Muyldermans, S., Baral, T.N., Retamozzo, V.C., De Baetselier, P., De Genst, E., Kinne, J., Leonhardt, H., Magez, S., Nguyen, V.K., Revets, H., Rothbauer, U., Stijlemans, B., Tillib, S., Wernery, U., Wyns, L., Hassanzadeh-Ghassabeh, G., Saerens, D., 2009. Camelid immunoglobulins and nanobody technology. Vet. Immunol. Immunopathol. 128, 178–183.

Paciucci, R., Vila, M.R., Adell, T., Diaz, V.M., Tora, M., Nakamura, T., Real, F.X., 1998. Activation of the urokinase plasminogen activator/urokinase plasminogen activator receptor system and redistribution of E-cadherin are associated with hepatocyte growth factor-induced motility of pancreas tumor cells overexpressing Met. Am. J. Pathol. 153, 201–212.

Petersen, H.H., Hansen, M., Schousboe, S.L., Andreasen, P.A., 2001. Localization of epitopes for monoclonal antibodies to urokinase-type plasminogen activator—relationship between epitope localization and effects of antibodies on molecular interactions of the enzyme. Eur. J. Biochem. 268, 4430–4439.

Rabbani, S.A., Xing, R.H., 1998. Role of urokinase (uPA) and its receptor (uPAR) in invasion and metastasis of hormone-dependent malignancies. Int. J. Cancer 12, 911–920.

Rahbarizadeh, F., Rasaee, M.J., Forouzandeh, M., Allameh, A.A., 2006. Over expression of anti-MUC1 single-domain antibody fragments in the yeast *Pichia pastoris*. Mol. Immunol. 43, 426–435.

Rath, S., Stanley, C.M., Steward, M.W., 1988. An inhibition enzyme-immunoassay for estimating relative antibody-affinity and affinity heterogeneity. J. Immunol. Methods 106, 245–249.

Renatus, M., Bode, W., Huber, R., Sturzebecher, J., Stubbs, M.T., 1998. Structural and functional analyses of benzamidine-based inhibitors in complex with trypsin: implications for the inhibition of factor Xa, tPA, and urokinase. J. Med. Chem. 41, 5445–5456.

Revets, H., De Baetselier, P., Muyldermans, S., 2005. Nanobodies as novel agents for cancer therapy. Expert Opin. Biol. Ther. 5, 111–124.

Roovers, R.C., Laeremans, T., Huang, L., De Taeye, S., Verkleij, A.J., Revets, H., de Haard, H.J., van Bergen en Henegouwen, P.M., 2007. Efficient inhibition of EGFR signaling and of tumour growth by antagonistic anti-EFGR Nanobodies. Cancer Immunol. Immunother. 56, 303–317.

Sgier, D., Zuberbuehler, K., Pfaffen, S., Neri, D., 2010. Isolation and characterization of an inhibitory human monoclonal antibody specific to the urokinase-type plasminogen activator, uPA. Protein Eng., Des. Sel. 23, 261–269.

Shahi, B., Mousavi Gargari, S.L., Rasooli, I., Rajabi Bazl, M., Hoseinpoor, R., 2014. Random mutagenesis of BoNT/E Hc nanobody to construct a secondary phage-display library. J. Appl. Microbiol. 117, 528–536.

Sircar, A., Sanni, K.A., Shi, J., Gray, J.J., 2011. Analysis and modeling of the variable region of camelid single-domain antibodies. J. Immunol. 186, 6357–6367.

Skottrup, P.D., Leonard, P., Kaczmarek, J.Z., Veillard, F., Enghild, J.J., O'Kennedy, R., Sroka, A., Clausen, R.P., Potempa, J., Riise, E., 2011. Diagnostic evaluation of a nanobody with picomolar affinity toward the protease RgpB from *Porphyromonas gingivalis*. Anal. Biochem. 415, 158–167.

Sperl, S., Jacob, U., de Prada, N.A., Sturzebecher, J., Wilhelm, O.G., Bode, W., Magdolen, V., Huber, R., Moroder, L., 2000. (4-Aminomethyl)phenylguanidine derivatives as nonpeptidic highly selective inhibitors of human urokinase. Proc. Natl. Acad. Sci. U.S.A. 97, 5113–5118.

Spraggon, G., Phillips, C., Nowak, U.K., Ponting, C.P., Saunders, D., Dobson, C.M., Stuart, D.I., Jones, E.Y., 1995. The crystal structure of the catalytic domain of human urokinase-type plasminogen activator. Structure 3, 681–691.

Thanongsaksrikul, J., Srimanote, P., Maneewatch, S., Choowongkomon, K., Tapchaisri, P., Makino, S., Kurazono, H., Chaicumpa, W., 2010. A V H H that neutralizes the zinc metalloproteinase activity of botulinum neurotoxin type A. J. Biol. Chem. 285, 9657–9666.

Thomassen, Y.E., Verkleij, A.J., Boonstra, J., Verrips, C.T., 2005. Specific production rate of VHH antibody fragments by *Saccharomyces cerevisiae* is correlated with growth rate, independent of nutrient limitation. J. Biotechnol. 118, 270–277.

van der Vaart, J.M., 2002. Expression of VHH antibody fragments in *Saccharomyces cerevisiae*. Methods Mol. Biol. 178, 359–366.

Vincenza Carriero, M., Franco, P., Vocca, I., Alfano, D., Longanesi-Cattani, I., Bifulco, K., Mancini, A., Caputi, M., Stoppelli, M.P., 2009. Structure, function and antagonists of urokinase-type plasminogen activator. Front. Biosci. 1, 3782–3794.

Zeslawska, E., Schweinitz, A., Karcher, A., Sondermann, P., Sperl, S., Sturzebecher, J., Jacob, U., 2000. Crystals of the urokinase type plasminogen activator variant beta c-uPA in complex with small molecule inhibitors open the way towards structure-based drug design. J. Mol. Biol. 301, 465–475.